ACS OMEGA
http://pubs.acs.org/journal/acsodf Article

Strain-Induced Modulation of Resistive Switching Temperature in Epitaxial VO_2 Thin Films on Flexible Synthetic Mica

Yuta Arata,* Hiroyuki Nishinaka,* Minoru Takeda, Kazutaka Kanegae, and Masahiro Yoshimoto

Cite This: ACS Omega 2022, 7, 41768–41774

Read Online

ACCESS | Metrics & More | Article Recommendations

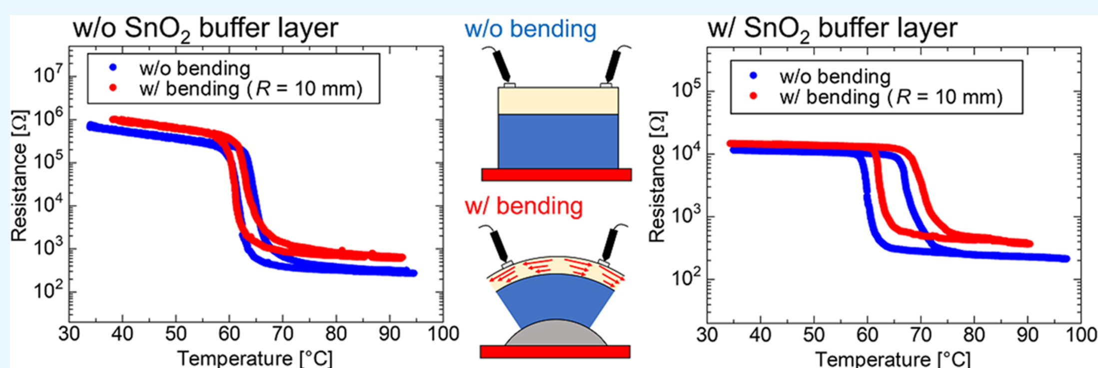

ABSTRACT: The resistive switching temperature associated with the metal−insulator transition (MIT) of epitaxial VO_2 thin films grown on flexible synthetic mica was modulated by bending stress. The resistive switching temperature of polycrystalline VO_2 and V_2O_5 thin films, initially grown on synthetic mica without a buffer layer, was observed not to shift with bending stress. By inserting a SnO_2 buffer layer, epitaxial growth of the VO_2 (010) thin film was achieved, and the MIT temperature was found to vary with the bending stress. Thus, it was revealed that the bending response of the VO_2 thin film depends on the presence or absence of the SnO_2 buffer layer. The bending stress applied a maximum in-plane tensile strain of 0.077%, resulting in a high-temperature shift of 2.3 °C during heating and 1.8 °C during cooling. After 10^4 bending cycles at a radius of curvature R = 10 mm, it was demonstrated that the epitaxial VO_2 thin film exhibits resistive switching temperature associated with MIT.

1. INTRODUCTION

Vanadium dioxide (VO_2), exhibiting a metal−insulator transition (MIT), has attracted attention as a promising material for oxide electronics. VO_2 has a monoclinic phase and is an insulator at room temperature, whereas it transforms to a metallic rutile phase at approximately 67 °C.[1,2] The phase transition of VO_2 is reversible and dramatically changes the electrical conductivity and infrared transmittance.[2−6] Furthermore, the MIT of VO_2 can be induced by various stimuli such as electricity,[7−9] light,[10,11] and strain[12,13] in addition to heat. Hence, VO_2 has been studied for applications in nonvolatile memory,[14−16] smart windows,[17−21] flexible strain sensors,[12] optical temperature sensors,[22] and gas sensors.[23]

One major research interest pertaining to VO_2 is to alter its MIT temperature. Various methods have been proposed to tune the MIT temperature. Doping has been reported to change the phase transition temperature of VO_2. Dopants like W, Mo, and Nb decrease the MIT temperature.[24−26] Conversely, dopants like Cr and Fe increase the MIT temperature.[27−29] Straining VO_2 thin films is also known to change its MIT temperature. For example, Breckenfeld et al. demonstrated that straining heterostructured VO_2/TiO_2 reduces its MIT temperature to ∼44 °C.[30] Kim et al. reported that a 50 nm epitaxial VO_2 thin film grown on a sapphire substrate with a SnO_2 (001) buffer layer reduced the transition temperature to 52 °C.[31] In addition, Muraoka and Hiroi studied the effect of uniaxial stress on the MIT of epitaxial VO_2 thin films grown on (001) and (110) TiO_2 substrates. As a result, they reported that the MIT temperature of VO_2 thin film grown on (001) TiO_2 decreases and that of VO_2 thin film grown on (110) TiO_2 increases.[32] Hong et al. investigated the in-plane strain directions using different orientations of VO_2 thin films on (001), (110), and (101) TiO_2 substrates and revealed that the MIT temperature depends on the strain state of the dimetric vanadium (V−V) atomic chain.[33] In particular, a compressive strain of V−V chains decreases MIT temperature, whereas a tensile strain increases MIT temperature.

Received: September 19, 2022
Accepted: October 21, 2022
Published: November 1, 2022

ACS Publications
© 2022 The Authors. Published by American Chemical Society

https://doi.org/10.1021/acsomega.2c06062
ACS Omega 2022, 7, 41768−41774

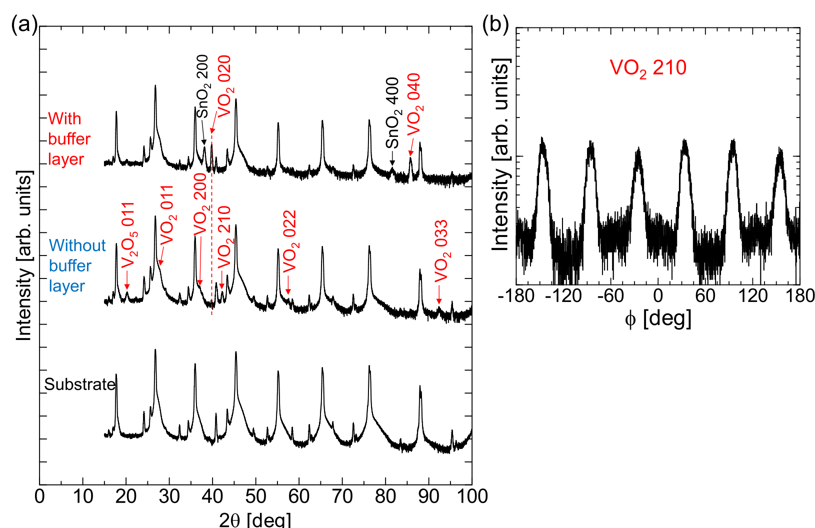

Figure 1. (a) XRD $2\theta-\omega$ scan profiles of VO_2 thin films grown on synthetic mica substrates with and without SnO_2 buffer layers. The scan profile of the synthetic mica substrate is included for reference. (b) XRD φ scan profile for the asymmetric (210) reflection of VO_2.

Epitaxial strain allows large MIT temperature modulation; however, the stress−strain relation is determined by the lattice mismatch with the substrate, and the stress cannot be altered after film formation. To alter the stress state (and consequently the MIT temperature), the deposited VO_2 could instead be deformed by bending and/or stretching. Cao et al. reported that the MIT temperature of VO_2 nanobeams could be altered by bending and stretching them.[34] However, the difficulty of bending single nanostructures is a barrier to their use in device applications.

Although it is challenging to induce bending stress in nanostructures because of their small size, it is relatively simple to induce bending stress in thin films because of their larger size. Thus, by growing single-crystal VO_2 thin films on flexible substrates, it would be possible to change the MIT temperature by straining them. In this study, we focused on van der Waals epitaxy as a technique for attaching VO_2 thin films to flexible substrates on muscovite mica and synthetic mica.[35,36] Mica is an inorganic two-dimensional (2D) material that can be thinned by mechanical cleavage. Although 2D materials have no dangling bonds at the cleavage surface, epitaxial thin films are grown by van der Waals epitaxy. Heteroepitaxial growth of various oxide thin films, such as VO_2,[36−38] MoO_2,[39] ZnO,[40,41] NiO,[42] In_2O_3,[42] Al-doped ZnO (AZO),[43] ε-Fe_2O_3,[44] and κ-Ga_2O_3,[45] on muscovite mica and synthetic mica has been previously demonstrated. Furthermore, it has been shown that inducing bending stress in epitaxial thin films grown by van der Waals epitaxy changes the resistivity of ZnO and the magnetic anisotropy of ε-Fe_2O_3.[40,44]

Mist chemical vapor deposition (CVD) was utilized to grow epitaxial VO_2 thin films on flexible synthetic mica. In previous studies, we have demonstrated van der Waals epitaxy of various oxides, such as ZnO,[41] NiO,[42] In_2O_3,[42] and κ-Ga_2O_3,[45] by mist CVD. In addition, VO_2 thin films grown on rigid quartz substrates by mist CVD had high visible transmittance and exhibited large changes in the infrared transmittance with MIT.[46] However, few reports exist on the epitaxial growth of VO_2 on flexible substrates using mist CVD. In this study, epitaxial VO_2 thin films were grown on flexible synthetic mica using van der Waals epitaxy via mist CVD and were then stressed by bending.

During the growth of VO_2 thin films, attention should be paid to the formation of V_2O_5, which is the most stable form of vanadium oxide.[47,48] Furthermore, since the strain along the dimeric V−V atomic chain affects the MIT temperature, epitaxial growth is necessary to modulate the properties of VO_2 thin films by bending stress. Therefore, to obtain the VO_2 thin film with desired orientation, we inserted SnO_2 as a buffer layer. SnO_2 has the same rutile structure as the metallic phase of VO_2.[49] SnO_2 has previously been utilized as a buffer layer for the epitaxial growth of VO_2.[31] The epitaxial growth of highly crystalline SnO_2 thin films on sapphire substrates via mist CVD has also been reported.[50,51] Hence, to grow epitaxial VO_2 thin films, we proposed to utilize SnO_2 buffer layers on synthetic mica. In this study, VO_2 thin films were grown on synthetic mica with and without SnO_2 buffer layers by mist CVD, and their electrical properties and MIT behavior were subsequently investigated. Furthermore, to clarify the effect of bending-induced in-plane tensile strain on the resistive switching temperature, the electrical characteristics of the VO_2 thin films were measured in the bent state.

2. RESULTS AND DISCUSSION

A (010) VO_2 layer was first grown on the synthetic mica substrate containing a (100) SnO_2 buffer layer. Figure 1a shows X-ray diffraction (XRD) $2\theta-\omega$ scan profiles of VO_2 thin films grown on synthetic mica substrates with and without SnO_2 buffer layers. For reference, the $2\theta-\omega$ scan profile of the synthetic mica substrate is depicted in Figure 1a. The diffraction peaks corresponding to the (011), (010), (100), and (210) planes of monoclinic VO_2 were observed when the SnO_2 buffer layer was absent. In addition to this, the diffraction peak of the (011) plane of tetragonal V_2O_5 was also observed. Thus, in the absence of a SnO_2 buffer layer, the deposited polycrystalline thin film consisted of a mixture of VO_2 and V_2O_5. On the other hand, diffraction peaks corresponding to the (010) plane of VO_2 and the (100) plane of SnO_2 were observed when the SnO_2 buffer layer was present, indicating that (010)-oriented monoclinic VO_2 was grown on the (100)-oriented SnO_2 buffer layer. To investigate the in-plane orientation of the VO_2 (010) thin film, we performed φ scanning of the VO_2 {210} reflection with the buffer layer, as

https://doi.org/10.1021/acsomega.2c06062
ACS Omega 2022, 7, 41768−41774

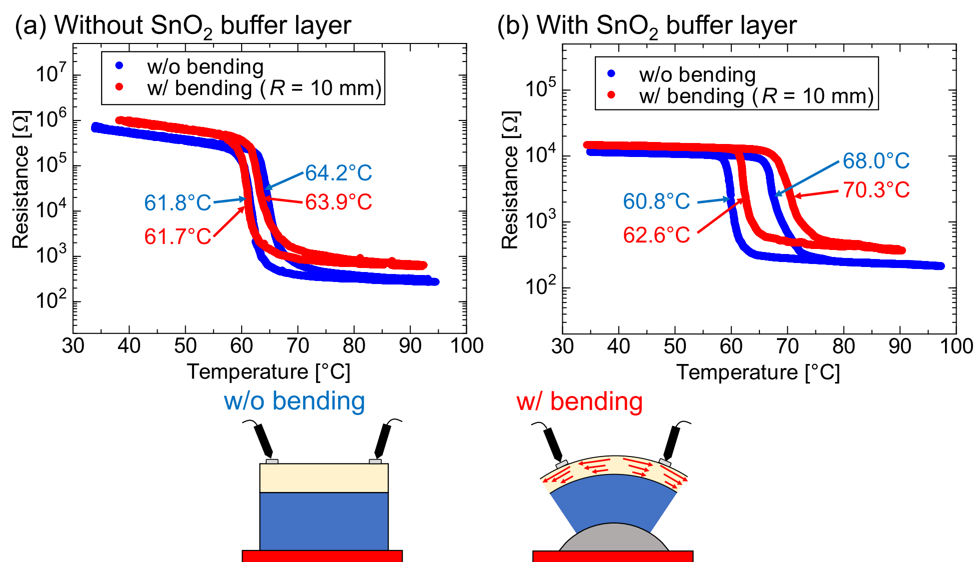

Figure 2. Variation of the electrical resistance of VO_2 thin films grown (a) without and (b) with a buffer layer with temperature. The blue and red dots indicate the properties of the sample in unbent and bent states, respectively, at a radius of curvature of 10 mm. The values of the transition temperatures for each state are also highlighted. Schematics of measurements without and with bending are also shown.

shown in Figure 1b. Six diffraction peaks were observed at intervals of 60°, indicating that the VO_2 thin film exhibited a fixed in-plane orientation unlike a randomly oriented polycrystal. Thus, by inserting the SnO_2 buffer layer, epitaxial VO_2 thin film could be successfully grown on synthetic mica by mist CVD.

Next, we investigated impacts of the buffer layer and bending stress on the MIT characteristics of VO_2 thin films. Figure 2 shows the electrical resistance of VO_2 thin films grown without and with buffer layers as a function of temperature. First, we discuss the difference in MIT characteristics due to the presence of the buffer layer. The temperature dependence of the electrical resistance of VO_2 thin films without bending stress is indicated by the blue dots in Figure 2. The MIT temperatures calculated from the peaks of the derivative curves of the relationship between the sample temperature and the electrical resistance are also highlighted in Figure 2. The resistive switching derived from the MIT was observed in both VO_2 thin films with and without a buffer layer. The resistive change of MIT with the buffer layer was smaller than without the buffer layer. This is because the SnO_2 buffer layer has higher conductivity than the insulator phase of VO_2, resulting in lower resistance below the MIT temperature than without the buffer layer. On the other hand, although both thin films showed hysteresis during the cooling and heating processes, their MIT temperatures were different. The MIT temperatures of the VO_2 thin film without the buffer layer were 64.2 °C during heating and 61.8 °C during cooling, whereas those of the thin film with the buffer layer were 68.0 °C during heating and 60.8 °C during cooling. We believe that this difference may be due to smaller crystallites in the polycrystalline thin film and larger crystallites in the epitaxial thin film.[52]

Now, we discuss the impact of bending stress on the MIT characteristics of VO_2 thin films. We utilized a brass rod with a radius of 10 mm to bend the thin films. The red dots in Figure 2 correspond to the measured resistances of the bent films. A shift in the resistive switching temperature was more prominently observed in the epitaxial VO_2 thin film with the buffer layer than in the polycrystalline VO_2 thin film without the buffer layer. The shift due to bending was higher by 2.3 °C during heating and 1.8 °C during cooling. By stretching VO_2 nanobeams and applying epitaxial strain to VO_2 thin films, it has been reported that tensile strain along the *a*-axis increases the MIT temperature of monoclinic VO_2.[32−34] On the other hand, as shown in Figure 1b, the epitaxial VO_2 (010) thin film grown on the synthetic mica formed three domains. By bending in one direction, the tensile strain can be applied to the *a*-axis direction of each VO_2 domain as long as it is not perpendicular to the bending direction. The strain effect is not canceled, and all domains stretched along the *a*-axis lead to an increase in the MIT temperature. Therefore, epitaxial VO_2 (010) thin films with three domains increased MIT temperature due to bending stress. Our result depicting a shift of the MIT temperature of the epitaxial VO_2 (010) thin film to a higher temperature by applying in-plane tensile strain through bending is consistent with these reports. Since the VO_2 thin film without the buffer layer was randomly oriented, the *a*-axis strain was not perfectly aligned along the bending direction, and the shift in MIT temperature derived from the strain was not significant. Thus, it was demonstrated that the MIT temperature of the epitaxial VO_2 thin film containing a SnO_2 buffer layer grown on a mica substrate could be altered by bending it.

We varied the amount of bending of the thin films to investigate the impact of bending stress on the MIT temperature. For a sample with thickness t bent at a radius of curvature R, the in-plane strain ε developed on the thin film surface is

$$\varepsilon = \frac{t}{2R} \tag{1}$$

Figure 3 shows the variation in the MIT temperature of the VO_2 thin film grown on synthetic mica with the buffer layer as a function of the in-plane tensile strain ε. Herein, the red and blue dots indicate the transition temperatures during heating and cooling, respectively. As the in-plane tensile strain increases, the MIT temperature of VO_2 gradually increases.

https://doi.org/10.1021/acsomega.2c06062
ACS Omega 2022, 7, 41768−41774

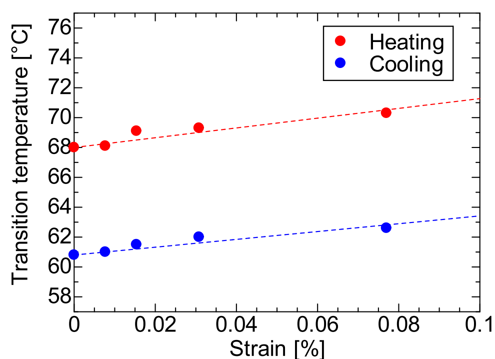

Figure 3. Variation of MIT temperature with in-plane tensile strain of the bent epitaxial film during heating and cooling.

For example, the application of an in-plane tensile strain of 0.077% increased the MIT temperature by 2.3 °C during heating and 1.8 °C during cooling. Moreover, the MIT temperature of the VO_2 thin film on the mica substrate was observed to vary linearly with the tensile strain. Assuming that such a linear relationship is valid even at larger strains, a 1% in-plane compressive strain can be expected to lower the MIT temperature by 32.7 °C during heating and 26.2 °C during cooling, allowing MIT to occur at room temperature.

To investigate the bending endurance, the epitaxial VO_2 thin film on the mica substrate was repeatedly bent, and the MIT temperature was measured in the unbent state. The bending tests were performed for 1−10^4 cycles with a radius of curvature of 10 mm. Figure 4a,b shows the MIT temperature of the epitaxial VO_2 thin film during heating and cooling and the electrical resistance at 40 °C (the insulating phase) and 80 °C (the metallic phase), respectively, in the unbent state after bending. After the bending test, the transition temperature was maintained during both heating and cooling cycles in the unbent state. Furthermore, the electrical resistance of the epitaxial VO_2 thin film remained more or less constant with bending cycles, as shown in Figure 4b. Figure 4c shows the temperature dependence of the electrical resistance of the epitaxial VO_2 thin film after 10^4 bending cycles. Herein, the blue and red dots indicate the measurements performed without and with bending, respectively, at a radius of curvature of 10 mm. After 10^4 bending cycles, the temperature-dependent MIT behavior without and with bending was mostly maintained. These results indicate that the epitaxial VO_2 thin film on synthetic mica exhibits high bending durability.

Raman scattering measurements were performed to investigate the effect of in-plane strain due to bending. We focused on the peak wavenumber at 607 cm^{-1}, corresponding to the V−O bond vibration, which has been reported to exhibit a continuously higher wavenumber shift due to tensile strain along the *a*-axis of monoclinic VO_2.[53,54] We analyzed the peak wavenumber shift of V−O phonons with in-plane tensile strain due to bending at different radii of curvature by measuring the Raman scattering. Figure 5a shows the Raman spectra in the range of 590−630 cm^{-1} under various strains of the VO_2 thin film epitaxially grown on synthetic mica. Figure 5b shows the variation of the V−O phonon peak wavenumber and the in-plane tensile strain by bending. The V−O phonon with a peak at 607 cm^{-1} in the unbent state was shifted to a higher wavenumber as the tensile strain of the thin film increased.

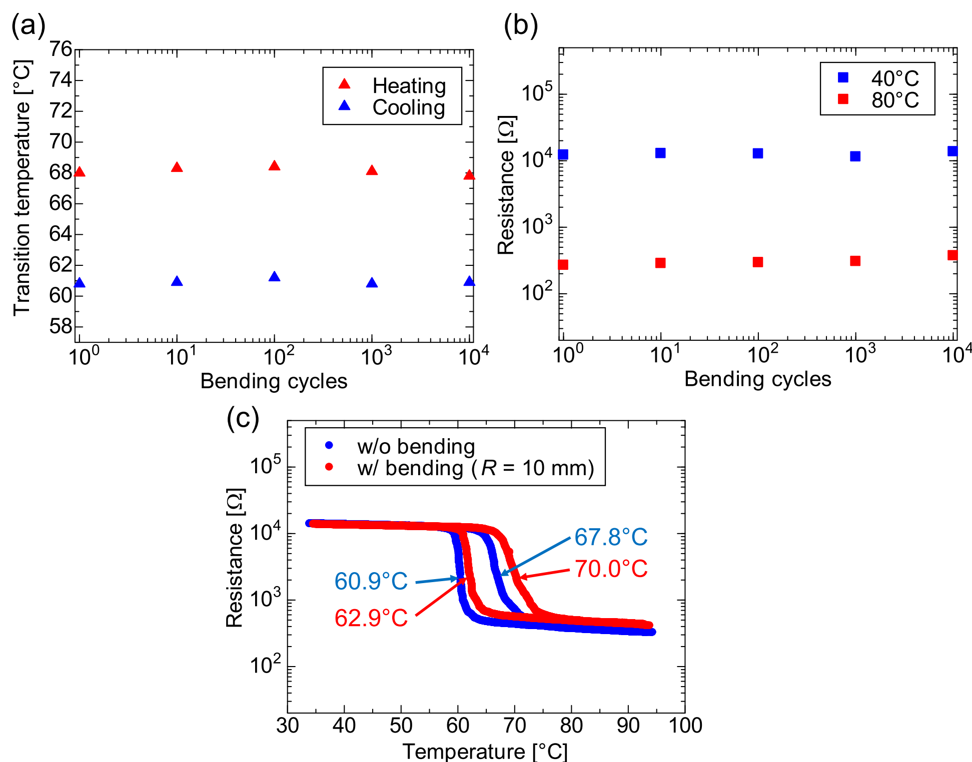

Figure 4. Variation in (a) the transition temperature of the unbent epitaxial VO_2 thin film on synthetic mica with a SnO_2 buffer layer upon heating and cooling and (b) the electrical resistance of the thin film at 40 and 80 °C as a function of bending cycles. (c) Variation in the electrical resistance of the epitaxial VO_2 thin film as a function of temperature after 10^4 bending cycles. The radius of curvature in the bent state was R = 10 mm. The transition temperature values with and without bending are also shown.

https://doi.org/10.1021/acsomega.2c06062
ACS Omega 2022, 7, 41768−41774

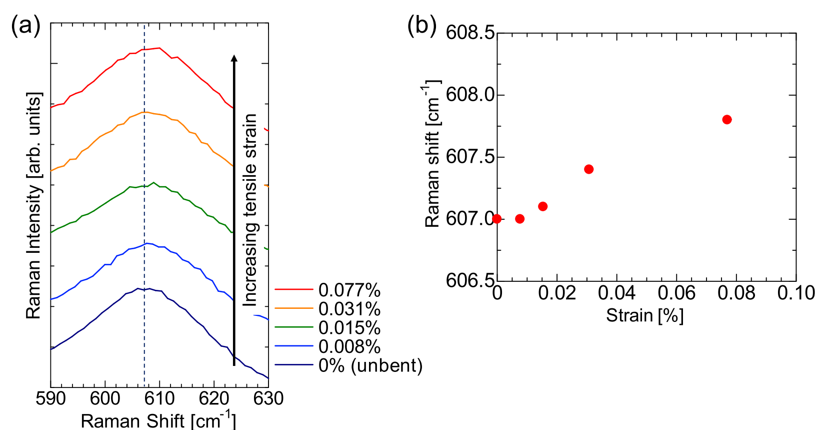

Figure 5. (a) Raman spectra of the epitaxial VO_2 thin film grown on synthetic mica with a SnO_2 buffer layer in the unbent state. The dashed line indicates the V−O phonon peak in the unbent state. (b) Variation of the peak wavenumber of V−O phonons (607 cm^{-1} without bending) with in-plane tensile strain due to bending.

Atkin et al. reported shifts toward larger V−O phonons with tensile strains (0−2%) applied to the VO_2 microbeam,[53] which is consistent our observations. The peak wavenumber of the V−O phonon exhibited a shift of 0.8 cm^{-1} due to an in-plane tensile strain of 0.077%. Thus, the stress induced by bending in the epitaxial VO_2 thin film caused the V−O phonon shift.

3. CONCLUSIONS

Epitaxial VO_2 thin films were grown on flexible synthetic mica with a SnO_2 buffer layer utilizing mist CVD. Focusing on the electrical properties of the VO_2 thin film, the resistive switching temperature associated with the MIT was modulated by bending stress. The polycrystalline VO_2 and V_2O_5 thin films grown without a SnO_2 buffer layer showed no modulation of the MIT temperature by bending. On the other hand, the epitaxial VO_2 thin film grown by inserting a SnO_2 buffer layer exhibited a shift in MIT temperature due to the tensile strain along the *a*-axis direction. Therefore, the effect of bending stress on VO_2 thin films grown on flexible synthetic mica can be altered with a SnO_2 buffer layer. The resistive switching temperature could be continuously modulated by varying the bending-induced in-plane tensile strain applied to the epitaxial VO_2 thin film. Even after 10^4 bending cycles, the epitaxial VO_2 thin film exhibited MIT and a shift in resistive switching temperature due to the in-plane tensile strain, demonstrating excellent bending durability. Raman measurements also demonstrated that tensile strain applied to the VO_2 thin film with a SnO_2 buffer layer induced bending stress. These results are expected to promote further development of strain engineering for epitaxial VO_2 thin films and their application to flexible switching devices.

4. METHODS

The epitaxial growth of VO_2 thin films and the insertion of a SnO_2 buffer layer by mist CVD were demonstrated using cleaved flexible synthetic mica as a substrate. The synthetic mica substrate surface obtained by cleavage was fresh and did not require cleaning to remove contamination. Tin(IV) chloride pentahydrate ($SnCl_4{\cdot}5H_2O$) was utilized as the Sn precursor and dissolved in a mixture of de-ionized water and hydrochloric acid (HCl). Vanadyl acetylacetonate ($VO(C_5H_7O_2)_2$) was utilized as the V precursor and dissolved in de-ionized water. The concentrations of the Sn and V precursors were fixed at 0.5 and 0.03 M, respectively. The precursor solution was atomized by ultrasonic transducers (2.4 MHz) and transported by nitrogen (N_2) gas at a flow rate of 6.5 L/min during the growth of the SnO_2 buffer layer. During the growth of VO_2 thin films, the mist was transported by introducing oxygen (O_2) gas at a flow rate of 0.1 L/min and N_2 gas at a flow rate of 7.9 L/min. The respective growth temperature and time were 475 °C and 0.5 min for the SnO_2 buffer layer and 500 °C and 60 min for the VO_2 thin films.

The structural characterization of VO_2 thin films grown on synthetic mica with and without a SnO_2 buffer layer was performed by XRD (Bruker, D8 Discover) analysis using Cu Kα radiation as the X-ray source. The crystal structure and out-of-plane orientation were analyzed by XRD $2\theta-\omega$ scans, and the in-plane structure was characterized by a φ-scan. The resistive switching associated with the MIT of VO_2 thin films was demonstrated by two-terminal measurements, while measuring the sample temperature using K-type thermocouples. Ti/Au ohmic contacts were deposited on the thin film surface for electrical measurements using electron beam evaporation (ULVAC, CV-200). In addition, to analyze the resistance change characteristics of the bent film owing to MIT, electrical measurements were obtained by attaching samples to brass rods of different radii (R = 10, 25, 50, and 100 mm) using polyimide tape. The thickness of each layer required for strain estimation of the epitaxial VO_2 thin film was measured using a micrometer (Mitutoyo MDH-25MB) and a scanning electron microscope (SEM, Hitachi S-5200). The thickness values of the thin film with the buffer layer and the synthetic mica substrate were 440 nm and 15 μm, respectively. The bending endurance of the flexible VO_2 thin films was investigated by attaching the sample to an automated stage with a jig and evaluating its MIT behavior after repeated bending. The maximum number of bending cycles was 10^4. A laser Raman spectrophotometer (Nihon Spectroscopy, NRS-5100) was used to obtain the Raman spectra of the unbent and bent VO_2 epitaxial thin films. The excitation laser wavelength was 532 nm, and the output power was 0.6 mW.

■ AUTHOR INFORMATION

Corresponding Authors

Yuta Arata − *Department of Electronics, Kyoto Institute of Technology, Kyoto 606-8585, Japan;* orcid.org/0000-0003-3102-5625; Email: d0822001@edu.kit.ac.jp

https://doi.org/10.1021/acsomega.2c06062
ACS Omega 2022, 7, 41768−41774

Hiroyuki Nishinaka − *Faculty of Electrical Engineering and Electronics, Kyoto Institute of Technology, Kyoto 606-8585, Japan*; orcid.org/0000-0003-1878-0765; Email: nisinaka@kit.ac.jp

Authors

Minoru Takeda − *Faculty of Electrical Engineering and Electronics, Kyoto Institute of Technology, Kyoto 606-8585, Japan*

Kazutaka Kanegae − *Faculty of Electrical Engineering and Electronics, Kyoto Institute of Technology, Kyoto 606-8585, Japan*

Masahiro Yoshimoto − *Faculty of Electrical Engineering and Electronics, Kyoto Institute of Technology, Kyoto 606-8585, Japan*

Complete contact information is available at:
https://pubs.acs.org/10.1021/acsomega.2c06062

Author Contributions

The manuscript was written through contributions of all authors. All authors have given their approval of the final version of the manuscript.

Notes

The authors declare no competing financial interest.

■ ACKNOWLEDGMENTS

This study was supported by JST SPRING, Grant Number JPMJSP2107.

■ REFERENCES

(1) Goodenough, J. B. The Two Components of the Crystallographic Transition in VO_2. *J. Solid State Chem.* **1971**, *3*, 490−500.

(2) Morin, F. J. Oxides Which Show a Metal-to-Insulator Transition at the Neel Temperature. *Phys. Rev. Lett.* **1959**, *3*, 34−36.

(3) Balberg, I.; Trokman, S. High-Contrast Optical Storage in VO_2 Films. *J. Appl. Phys.* **1975**, *46*, 2111−2119.

(4) Kim, D. H.; Kwok, H. S. Pulsed Laser Deposition of VO_2 Thin Films. *Appl. Phys. Lett.* **1994**, *65*, 3188−3190.

(5) Livage, J. Optical and Electrical Properties of Vanadium Oxides Synthesized from Alkoxides. *Coord. Chem. Rev.* **1999**, *190*−*192*, 391−403.

(6) Borek, M.; Qian, F.; Nagabushnam, V.; Singh, R. K. Pulsed Laser Deposition of Oriented VO_2 Thin Films on *R*-Cut Sapphire Substrates. *Appl. Phys. Lett.* **1993**, *63*, 3288−3290.

(7) Stefanovich, G.; Pergament, A.; Stefanovich, D. Electrical Switching and Mott Transition in VO_2. *J. Phys.: Condens. Matter* **2000**, *12*, 8837−8845.

(8) Yang, Z.; Hart, S.; Ko, C.; Yacoby, A.; Ramanathan, S. Studies on Electric Triggering of the Metal-Insulator Transition in VO_2 Thin Films Between 77 K and 300 K. *J. Appl. Phys.* **2011**, *110*, No. 033725.

(9) Li, D.; Sharma, A. A.; Gala, D. K.; Shukla, N.; Paik, H.; Datta, S.; Schlom, D. G.; Bain, J. A.; Skowronski, M. Joule Heating-Induced Metal−Insulator Transition in Epitaxial VO_2/TiO_2 Devices. *ACS Appl. Mater. Interfaces* **2016**, *8*, 12908−12914.

(10) Wu, J. M.; Liou, L. B. Room Temperature Photo-induced Phase Transitions of VO_2 Nanodevices. *J. Mater. Chem.* **2011**, *21*, 5499−5504.

(11) Li, G.; Xie, D.; Zhong, H.; Zhang, Z.; Fu, X.; Zhou, Q.; Li, Q.; Ni, H.; Wang, J.; Guo, E. J.; He, M.; Wang, C.; Yang, G.; Jin, K.; Ge, C. Photo-induced Non-volatile VO_2 Phase Transition for Neuromorphic Ultraviolet Sensors. *Nat. Commun.* **2022**, *13*, No. 1729.

(12) Hu, B.; Ding, Y.; Chen, W.; Kulkarni, D.; Shen, Y.; Tsukruk, V. V.; Wang, Z. L. External-Strain Induced Insulating Phase Transition in VO_2 Nanobeam and Its Application as Flexible Strain Sensor. *Adv. Mater.* **2010**, *22*, 5134−5139.

(13) Hu, B.; Zhang, Y.; Chen, W.; Xu, C.; Wang, Z. L. Self-Heating and External Strain Coupling Induced Phase Transition of VO_2 Nanobeam as Single Domain Switch. *Adv. Mater.* **2011**, *23*, 3536−3541.

(14) Moatti, A.; Sachan, R.; Narayan, J. Volatile and Non-volatile Behavior of Metal−Insulator Transition in VO_2 Through Oxygen Vacancies Tunability for Memory Applications. *J. Appl. Phys.* **2020**, *128*, No. 045302.

(15) Fan, L.; Chen, Y.; Liu, Q.; Chen, S.; Zhu, L.; Meng, Q.; Wang, B.; Zhang, Q.; Ren, H.; Zou, C. Infrared Response and Optoelectronic Memory Device Fabrication Based on Epitaxial VO_2 Film. *ACS Appl. Mater. Interfaces* **2016**, *8*, 32971−32977.

(16) Velichko, A.; Pergament, A.; Putrolaynen, V.; Berezina, O.; Stefanovich, G. Effect of Memory Electrical Switching in Metal/Vanadium Oxide/Silicon Structures with VO_2 Films Obtained by the Sol−Gel Method. *Mater. Sci. Semicond. Process.* **2015**, *29*, 315−320.

(17) Cui, Y.; Ke, Y.; Liu, C.; Chen, Z.; Wang, N.; Zhang, L.; Zhou, Y.; Wang, S.; Gao, Y.; Long, Y. Thermochromic VO_2 for Energy-Efficient Smart Windows. *Joule* **2018**, *2*, 1707−1746.

(18) Gao, Y.; Luo, H.; Zhang, Z.; Kang, L.; Chen, Z.; Du, J.; Kanehira, M.; Cao, C. Nanoceramic VO_2 Thermochromic Smart Glass: A Review on Progress in Solution Processing. *Nano Energy* **2012**, *1*, 221−246.

(19) Zhou, J.; Gao, Y.; Zhang, Z.; Luo, H.; Cao, C.; Chen, Z.; Dai, L.; Liu, X. VO_2 Thermochromic Smart Window for Energy Savings and Generation. *Sci. Rep.* **2013**, *3*, No. 3029.

(20) Dietrich, M. K.; Kuhl, F.; Polity, A.; Klar, P. J. Optimizing Thermochromic VO_2 by Co-doping with W and Sr for Smart Window Applications. *Appl. Phys. Lett.* **2017**, *110*, No. 141907.

(21) Chang, T.; Zhu, Y.; Huang, J.; Luo, H.; Jin, P.; Cao, X. Flexible VO_2 Thermochromic Films with Narrow Hysteresis Loops. *Sol. Energy Mater. Sol. Cells* **2021**, *219*, No. 110799.

(22) Antunez, E. E.; Salazar-Kuri, U.; Estevez, J. O.; Campos, J.; Basurto, M. A.; Sandoval, S. J.; Agarwal, V. Porous Silicon-VO_2 Based Hybrids as Possible Optical Temperature Sensor: Wavelength-Dependent Optical Switching from Visible to Near-Infrared Range. *J. Appl. Phys.* **2015**, *118*, No. 134503.

(23) Strelcov, E.; Lilach, Y.; Kolmakov, A. Gas Sensor Based on Metal−Insulator Transition in VO_2 Nanowire Thermistor. *Nano Lett.* **2009**, *9*, 2322−2326.

(24) Peng, Z.; Jiang, W.; Liu, H. Synthesis and Electrical Properties of Tungsten-Doped Vanadium Dioxide Nanopowders by Thermolysis. *J. Phys. Chem. C* **2007**, *111*, 1119−1122.

(25) Ji, C.; Wu, Z.; Wu, X.; Feng, H.; Wang, J.; Huang, Z.; Zhou, H.; Yao, W.; Gou, J.; Jiang, Y. Optimization of Metal-to-Insulator Phase Transition Properties in Polycrystalline VO_2 Films for Terahertz Modulation Applications by Doping. *J. Mater. Chem. C* **2018**, *6*, 1722−1730.

(26) Li, D.; Li, M.; Pan, J.; Luo, Y.; Wu, H.; Zhang, Y.; Li, G. Hydrothermal Synthesis of Mo-Doped VO_2/TiO_2 Composite Nanocrystals with Enhanced Thermochromic Performance. *ACS Appl. Mater. Interfaces* **2014**, *6*, 6555−6561.

(27) Brown, B. L.; Lee, M.; Clem, P. G.; Nordquist, C. D.; Jordan, T. S.; Wolfley, S. L.; Leonhardt, D.; Edney, C.; Custer, J. A. Electrical and Optical Characterization of the Metal-Insulator Transition Temperature in Cr-Doped VO_2 Thin Films. *J. Appl. Phys.* **2013**, *113*, No. 173704.

(28) Victor, J. L.; Gaudon, M.; Salvatori, G.; Toulemonde, O.; Penin, N.; Rougier, A. Doubling of the Phase Transition Temperature of VO_2 by Fe Doping. *J. Phys. Chem. Lett.* **2021**, *12*, 7792−7796.

(29) Tan, X.; Liu, W.; Long, R.; Zhang, X.; Yao, T.; Liu, Q.; Sun, Z.; Cao, Y.; Wei, S. Symmetry-Controlled Structural Phase Transition Temperature in Chromium-Doped Vanadium Dioxide. *J. Phys. Chem. C* **2016**, *120*, 28163−28168.

(30) Breckenfeld, E.; Kim, H.; Burgess, K.; Charipar, N.; Cheng, S. F.; Stroud, R.; Piqué, A. Strain Effects in Epitaxial VO_2 Thin Films on Columnar Buffer-Layer TiO_2/Al_2O_3 Virtual Substrates. *ACS Appl. Mater. Interfaces* **2017**, *9*, 1577−1584.

https://doi.org/10.1021/acsomega.2c06062
ACS Omega 2022, 7, 41768−41774

(31) Kim, H.; Bingham, N. S.; Charipar, N. A.; Piqué, A. Strain Effect in Epitaxial VO_2 Thin Films Grown on Sapphire Substrates Using SnO_2 Buffer Layers. *AIP Adv.* **2017**, *7*, No. 105116.
(32) Muraoka, Y.; Hiroi, Z. Metal−Insulator Transition of VO_2 Thin Films Grown on TiO_2 (001) and (110) Substrates. *Appl. Phys. Lett.* **2002**, *80*, 583−585.
(33) Hong, B.; Yang, Y.; Hu, K.; Dong, Y.; Zhou, J.; Zhang, Y.; Zhao, W.; Luo, Z.; Gao, C. Strain Engineering on the Metal-Insulator Transition of VO_2/TiO_2 Epitaxial Films Dependent on the Strain State of Vanadium Dimers. *Appl. Phys. Lett.* **2019**, *115*, No. 251605.
(34) Cao, J.; Ertekin, E.; Srinivasan, V.; Fan, W.; Huang, S.; Zheng, H.; Yim, J. W. L.; Khanal, D. R.; Ogletree, D. F.; Grossman, J. C.; Wu, J. Strain Engineering and One-Dimensional Organization of Metal−Insulator Domains in Single-Crystal Vanadium Dioxide Beams. *Nat. Nanotechnol.* **2009**, *4*, 732−737.
(35) Koma, A. Van Der Waals Epitaxy-A New Epitaxial Growth Method for a Highly Lattice-Mismatched System. *Thin Solid Films* **1992**, *216*, 72−76.
(36) Li, C.-I.; Lin, J.-C.; Liu, H.-J.; Chu, M.-W.; Chen, H.-W.; Ma, C.-H.; Tsai, C.-Y.; Huang, H.-W.; Lin, H.-J.; Liu, H.-L.; Chiu, P.-W.; Chu, Y. -H. van der Waal Epitaxy of Flexible and Transparent VO_2 Film on Muscovite. *Chem. Mater.* **2016**, *28*, 3914−3919.
(37) Yan, J.; Huang, W.; Zhang, Y.; Liu, X.; Tu, M. Characterization of Preferred Orientated Vanadium Dioxide Film on Muscovite (001) Substrate. *Phys. Status Solidi (A)* **2008**, *205*, 2409−2412.
(38) Liu, Y.-X.; Cai, Y.; Zhang, Y.-S.; Deng, X.; Zhong, N.; Xiang, P.-H.; Duan, C.-G. Van Der Waals Epitaxy for High-Quality Flexible VO_2 Film on Mica Substrate. *J. Appl. Phys.* **2021**, *130*, No. 025301.
(39) Ma, C.-H.; Lin, J.-C.; Liu, H.-J.; Do, T. H.; Zhu, Y.-M.; Ha, T. D.; Zhan, Q.; Juang, J.-Y.; He, Q.; Arenholz, E.; Chiu, P.-W.; Chu, Y.-H. Van Der Waals Epitaxy of Functional MoO_2 Film on Mica for Flexible Electronics. *Appl. Phys. Lett.* **2016**, *108*, No. 253104.
(40) Yen, M.; Lai, Y. H.; Zhang, C. L.; Cheng, H. Y.; Hsieh, Y. T.; Chen, J. W.; Chen, Y. C.; Chang, L.; Tsou, N. T.; Li, J. Y.; Chu, Y. H. Giant Resistivity Change of Transparent ZnO/Muscovite Heteroepitaxy. *ACS Appl. Mater. Interfaces* **2020**, *12*, 21818−21826.
(41) Chen, H.-G.; Shih, Y.-H.; Wang, H.-S.; Jian, S.-R.; Yang, T.-Y.; Chuang, S.-C. Van Der Waals Epitaxial Growth of ZnO Films on Mica Substrates in Low-Temperature Aqueous Solution. *Coatings* **2022**, *12*, No. 706.
(42) Arata, Y.; Nishinaka, H.; Shimazoe, K.; Yoshimoto, M. Epitaxial Growth of Bendable Cubic NiO and In_2O_3 Thin Films on Synthetic Mica for p- and n-Type Wide-Bandgap Semiconductor Oxides. *MRS Adv.* **2020**, *5*, 1671−1679.
(43) Ke, S.; Xie, J.; Chen, C.; Lin, P.; Zeng, X.; Shu, L.; Fei, L.; Wang, Y.; Ye, M.; Wang, D. D. van der Waals Epitaxy of Al-Doped ZnO Film on Mica as a Flexible Transparent Heater with Ultrafast Thermal Response. *Appl. Phys. Lett.* **2018**, *112*, No. 031905.
(44) Amrillah, T.; Quynh, L. T.; Nguyen Van, C. N.; Do, T. H.; Arenholz, E.; Juang, J. Y.; Chu, Y. H. Flexible Epsilon Iron Oxide Thin Films. *ACS Appl. Mater. Interfaces* **2021**, *13*, 17006−17012.
(45) Arata, Y.; Nishinaka, H.; Tahara, D.; Yoshimoto, M. van der Waals Epitaxy of Ferroelectric ε-Gallium Oxide Thin Film on Flexible Synthetic Mica. *Jpn. J. Appl. Phys.* **2020**, *59*, No. 025503.
(46) Matamura, Y.; Ikenoue, T.; Miyake, M.; Hirato, T. Mist CVD of Vanadium Dioxide Thin Films with Excellent Thermochromic Properties Using a Water-Based Precursor Solution. *Sol. Energy Mater. Sol. Cells* **2021**, *230*, No. 111287.
(47) Song, G. Y.; Oh, C.; Sinha, S.; Son, J.; Heo, J. Facile Phase Control of Multivalent Vanadium Oxide Thin Films (V_2O_5 and VO_2) by Atomic Layer Deposition and Postdeposition Annealing. *ACS Appl. Mater. Interfaces* **2017**, *9*, 23909−23917.
(48) Liu, Y.; Liu, J.; Li, Y.; Wang, D.; Ren, L.; Zou, K. Effect of Annealing Temperature on the Structure and Properties of Vanadium Oxide Films. *Opt. Mater. Express* **2016**, *6*, 1552−1560.
(49) Kim, K. H.; Chun, J. S. X-ray Studies of SnO_2 Prepared by Chemical Vapour Deposition. *Thin Solid Films* **1986**, *141*, 287−295.
(50) Okuno, T.; Oshima, T.; Lee, S.-D.; Fujita, S. Growth of SnO_2 Crystalline Thin Films by Mist Chemical Vapour Deposition Method. *Phys. Status Solidi (C)* **2011**, *8*, 540−542.
(51) Yatabe, Z.; Tsuda, T.; Matsushita, J.; Sato, T.; Otabe, T.; Sue, K.; Nagaoka, S.; Nakamura, Y. Single Crystalline SnO_2 Thin Films Grown on *m*-Plane Sapphire Substrate by Mist Chemical Vapor Deposition. *Phys. Status Solidi (C)* **2017**, *14*, No. 1600148.
(52) Suh, J. Y.; Lopez, R.; Feldman, L. C.; Haglund, R. F. Semiconductor to Metal Phase Transition in the Nucleation and Growth of VO_2 Nanoparticles and Thin Films. *J. Appl. Phys.* **2004**, *96*, 1209−1213.
(53) Atkin, J. M.; Berweger, S.; Chavez, E. K.; Raschke, M. B.; Cao, J.; Fan, W.; Wu, J. Strain and Temperature Dependence of the Insulating Phases of VO_2 near the Metal-Insulator Transition. *Phys. Rev. B.* **2012**, *85*, No. 020101(R).
(54) Evlyukhin, E.; Howard, S. A.; Paik, H.; Paez, G. J.; Gosztola, D. J.; Singh, C. N.; Schlom, D. G.; Lee, W. C.; Piper, L. F. J. Directly Measuring the Structural Transition Pathways of Strain-Engineered VO_2 Thin Films. *Nanoscale* **2020**, *12*, 18857−18863.